



OPEN The Kir channel in the nucleus tractus solitarius integrates the chemosensory system with REM sleep executive machinery for homeostatic balance

Fayaz A. Mir^{1,2} & Sushil K. Jha¹✉

The locus coeruleus (LC), nucleus tractus solitarius (NTS), and retrotrapezoid nucleus (RTN) are critical chemosensory regions in the brainstem. In the LC, acid-sensing ion channels and proton pumps serve as H⁺ sensors and facilitate the transition from non-rapid eye movement (NREM) to rapid eye movement (REM) sleep. Interestingly, the potassium inward rectifier (KIR) channels in the LC, NTS, and RTN also act as H⁺-sensors and are a primary target for improving sleep in obstructive sleep apnea and Rett syndrome patients. However, the role of Kir channels in NREM to REM sleep transition for H⁺ homeostasis is not known. Male Wistar rats were surgically prepared for chronic sleep–wake recording and drug delivery into the LC, NTS, and RTN. In different animal cohorts, microinjections of the Kir channel inhibitor, barium chloride (BaCl₂), at concentrations of 1 mM (low dose) and 2 mM (high dose) in the LC and RTN significantly increased wakefulness and decreased NREM sleep. However, BaCl₂ microinjection into the LC notably reduced REM sleep, whereas it didn't change in the RTN-injected group. Interestingly, BaCl₂ microinjections into the NTS significantly decreased wakefulness and increased the percent amount of NREM and REM sleep. Additionally, with the infusion of BaCl₂ into the NTS, the mean REM sleep episode numbers significantly increased, but the length of the REM sleep episode didn't change. These findings suggest that the Kir channels in the NTS, but not in the LC and RTN, modulate state transition from NREM to REM sleep.

Keywords Potassium inward rectifier channels, Hypercapnia, REM sleep, Locus coeruleus, Retrotrapezoid nucleus, Solitary tract nucleus, Chemosensory

Rapid eye movement (REM) sleep plays a crucial role in overall health, aiding in ionic homeostasis, brain development, endocrine regulation, and mental well-being^{1–5}. It features distinct physiological traits like increased breathing rate, heart rate, and EEG patterns similar to wakefulness⁶. Despite these physiological processes being energy-demanding, their heightened activity during REM sleep remains enigmatic^{7–9}. One reason for increased breathing rate during REM sleep could be that REM sleep might function as a sentinel to help maintain normal CO₂ levels during sleep⁷. Extended NREM sleep may cause hypoventilation and increased pCO₂ levels⁷. By regulating CO₂ levels, REM sleep possibly prevents physiological disruptions leading to frequent arousal and fragmented sleep^{1,7}. Frequent arousals or fragmented sleep are pathological conditions that can lead to various physiological diseases, including cardiorespiratory disorders¹⁰. Hence, one of the potential functions of REM sleep could be to facilitate uninterrupted, restorative sleep by regulating bodily CO₂ levels within the normal range, thereby enhancing overall well-being.

The central chemosensory system, comprising neuronal groups in the locus coeruleus (LC), Nucleus tractus solitarius (NTS), and retrotrapezoid nucleus (RTN), plays a crucial role in regulating breathing in response to changes in pH and CO₂ levels^{7,11–14}. The LC is important for integration of altered CO₂/pH with breathing modulation, but the NTS and RTN contribute significantly to this chemoregulatory mechanism. Localized acidification of these brainstem areas, using microinjection of acetazolamide or acidic cerebrospinal fluid

¹School of Life Sciences, Jawaharlal Nehru University, New Delhi 110067, India. ²Department of Anesthesia, Critical Care & Pain Medicine, Massachusetts General Hospital, Harvard Medical School, Boston, MA 02129, USA. ✉email: sushilkjha@mail.jnu.ac.in; sushil_1000@yahoo.com

infusion, notably increases breathing frequency and tidal volume^{12,14–18}. Furthermore, experiments involving lesions of these central chemosensory brain regions have shown that they are essential for the adaptive respiratory response during hypercapnia^{12,14,19–21}. For instance, in rats with kainic acid-induced RTN lesions, while normal breathing patterns remained unaffected, the response to hypercapnia was significantly diminished²². Recent studies targeting a substantial portion of Phox2b NTS neurons have revealed an increased threshold to apnea without altering overall CO₂ sensitivity^{19,21,23}. In contrast, lesions of the LC or genetic deletion of the dopamine beta-hydroxylase (DBH) enzyme result in profound impairments in hypercapnic responses, regular breathing, and heart rate regulation^{18,24}. Moreover, such changes can lead to breathing problems during sleep, which may accompany hypotension^{18,24}.

The chemosensory machinery also influences sleep–wake architecture. Studies suggest that the LC and RTN are involved in maintaining arousal^{12,25–27}. Activation of the LC and RTN neurons through electrical, chemical, and optogenetic stimulation increases wakefulness, whereas their inhibition induces sleep^{27–30}. Conversely, the NTS may promote sleep, particularly REM sleep, as most of the NTS neurons are active during REM sleep^{31,32}. A low threshold electrical stimulation of the central NTS increases theta and alpha waves and REM sleep¹³. Interestingly, the recurrence of REM sleep increases under a mild hypercapnic (2–4% CO₂) condition^{11,33}. The proton pumps and acid-sensing ion channels (ASICs) in the LC are pivotal in mediating the repeated recurrence of REM sleep and initiating the transition from non-rapid eye movement (NREM) to REM sleep states^{1,11,34}. These studies suggest that altering the brain's hydrogen ions, and chemosensory machinery influences either REM sleep or the state transition from NREM to REM sleep. Several receptors and channels, including Kir channels, play an essential role in maintaining hydrogen ion homeostatic balance in the brain^{11,34,35}. Kir channels play a crucial role in resetting neuronal membrane potential during pH fluctuations³⁶. Kir channels are abundantly expressed in the LC, NTS, and RTN neurons^{35–39}, and overexpression of Kir 4.1/4.5 channels in the LC alters hypercapnia-induced breathing responses, as is noticed in the Rett syndrome³⁷. However, the role of Kir channels in the modulation of S-W and sleep state transition from NREM to REM sleep is not known. We hypothesize that the Kir channel in the chemosensory neurons of the LC, NTS, and RTN could have a critical role in promoting the transition from NREM to REM sleep, ensuring smooth and uninterrupted sleep. This mechanism might be essential for maintaining sleep continuity and overall sleep quality.

Materials and methods

Animals

We have used male Wistar rats (n = 20) weighing 250–300 g. The animals were obtained from the Central Laboratory Animal Resources (CLAR) facility and taken to the department's animal room facility. They were kept for one week of habituation. The animals were maintained in a 12-h light–dark (L:D) cycle with lights on at 07:00 AM and off at 07:00 PM. The room temperature was maintained at 23 ± 1 °C. Food and water were given ad libitum. All animals, procedures, and protocols used in this study were approved by the Institutional Animal Ethical Committee (IAEC Protocol # 14/2015) of Jawaharlal Nehru University, New Delhi, India. Furthermore, all the experiments were performed under relevant guidelines and regulations, and data reporting in the manuscript follows the recommendations in the ARRIVE guidelines 2.0. We have made our best efforts to minimize the pain and discomfort of the animals and the number of animals used in the experiments.

Surgical procedures for polysomnographic recording and cannula implantation for microinjection of drugs in the LC, NTS, and RTN

Rats were randomly divided into three groups: (i) the LC group, (ii) the NTS group, and (iii) the RTN group. All animals were surgically prepared for chronic sleep–wakefulness (S-W) recording (for details, see Mir and Jha 2021)¹¹. Under sterile conditions, the animal was anesthetized by inhalation of isoflurane anesthesia (Baxter Healthcare, India) with 4% initiation and 0.5–2% maintenance using a facemask. The head was shaved and cleaned with iodine, followed by ethanol. The animal's head was fixed in stereotaxic apparatus (RWD Life Science, China), and a midline incision was made with a sterile surgical blade. The skin was moved aside to expose the skull for electrode implantation. Two pairs of small, stainless-steel screw electrodes were affixed on the skull above the frontal and parietal cortices to record electroencephalogram (EEG). Three electrodes (flexible insulated wires except at the tip) were implanted in the dorsal neck muscles to record bipolar electromyogram (EMG) (a third EMG was implanted as a safeguard). One stainless steel screw electrode was fixed laterally to the midline in the nasal bone as a reference electrode. A pair of bilateral stainless-steel cannulas for drug/vehicle infusions was implanted into the LC (at brain co-ordinate from bregma: –9.8 mm, 1.3 ML, DV 6 from skull surface) in the LC group of animals; in the NTS (at brain co-ordinate from bregma: –13.5 mm from bregma, 0.8 mm ML, DV 7.5 mm) in the NTS group of animals and in the RTN (at brain co-ordinate from bregma: –11.8 mm from bregma, 1.6 ML, DV 10.5 mm) in the RTN group of animals respectively. An obturator (blocker wire) was inserted into the guide cannula to prevent occlusion and blocking of the guide cannula. Free ends of EEG, EMG, and reference electrodes were connected to a 9-pin miniature connector, which was cemented onto the skull with dental acrylic cement. Finally, the neck skin was sutured. The animal was removed from the stereotaxic apparatus. The animal was kept on a heating pad and observed closely until it emerged from the anesthesia. An oral analgesic (Ibugesic Plus) was given to the animal for pain management. The animal received post-operative treatment for 3–4 consecutive days with intraperitoneal injections of dexamethasone (1.5 mg/kg) and gentamicin (2 mg/kg), along with the application of nebaself powder (an antibiotic) on the suture site to minimize brain inflammation and prevent infection. After the recovery period from surgery, the animal underwent acclimatization to the recording setup, experimental handling, and mock microinjections to minimize stress during subsequent experiments.

Experimental procedures (drug infusions)

We studied the effects of the Kir channel blocker Barium Chloride (BaCl_2), for which two different doses of the drug, low dose (1 mM) and high dose (2 mM), were used (based on reported IC_{50} values of the drug). Freshly prepared drug solutions and sterile saline (0.9%) were made, and a 200 nl volume was microinjected into each side of the LC, NTS, or RTN brain areas in their respective groups of animals. All drug doses and the respective vehicle solution were microinjected into the respective brain areas randomly on alternative days before sleep–wake recording. We kept a two-day interval between the low and high-dose microinjections to ensure complete clearance of the drug from the previous injection. BaCl_2 (Sigma Aldrich) at a low dose of 1 mM and a high dose of 2 mM was dissolved in 0.9% saline, and the pH was adjusted to 7.4. Then 200 nl of this solution was microinjected on each side (200 nl /side) into the respective nuclei over two min. The microinjection of nano volume over two minutes was chosen to restrict the diffusion within the nuclei. For the vehicle injection, 0.9% saline was microinjected in the same manner as the drug.

Polysomnographic recordings

After recovery from the surgery, rats were habituated for 2–3 days in a well-ventilated, and sound-dampened sleep recording chamber (black-colored plexiglass, size: 48" × 24" × 24"; illuminated with 40 Lux light). The animal was provided with food and water ad libitum. During the habituation days (Days 1 and 2), the animal was tethered to the recording cable from 11:00 AM to 5:00 PM daily to acclimatize the animals to the setup. The EEG and EMG signals were examined in a computer using "Somnologica Science" software and Embla A10 Medcare Flaga, Iceland. On the subsequent two days, Day 3 and 4, the animal was tethered to the recording cable, and two baselines of S–W were recorded for 6 h (11:00 AM to 5:00 PM). On days 5, 6, and 7, sleep–wake cycles were recorded following microinjections of either a vehicle, a low dose, or a high dose of BaCl_2 in a random order for 6 h (11:00 AM to 5:00 PM). Microinjections were always performed after a gap of two days between two drug injections in a randomized fashion to allow the clearance of the drug traces from the brain. EEG signals were recorded using high-pass (0.1 Hz) and low-pass (40 Hz) filters, while EMG signals were recorded with high-pass (10 Hz) and low-pass (90 Hz) filters, all digitized at a 100 Hz sampling rate. All recordings were saved and analyzed offline.

Microinjection procedure for drug infusion

The BaCl_2 solution was freshly prepared before injection at the desired concentration and adjusted to 7.4 pH. Before microinjection, animals were manually restrained, and the blocker wires of the cannula were removed and replaced with the injector cannula (30-gauge; 18 mm in length), which was connected to a short silicone tubing, further linked to the microinjector Hamilton syringe (10 μl ; Kent Scientific, USA). The injector cannula was inserted 1 mm beyond the tip of the guide cannula to ensure contact with the dorsal surface of the targeted site for drug/vehicle delivery. Subsequently, 200 nl of vehicle (0.9% saline) or BaCl_2 solution (low dose: 1 mM or high dose: 2 mM) was injected over 2 min at a 100 nl/min flow rate. The injector needle remained in the guide cannula for an additional 2 min before being slowly withdrawn, and blocker wires were reinserted into the guide cannula. Following microinjections, animals were promptly subjected to polysomnographic recording.

Histological identification of cannula and injector sites

After the completion of all experiments, the rats were sacrificed with an overdose of thiopentone anesthesia (80 mg/kg) and perfused transcardially with 0.9% saline and 10% formalin solution for 15 min each. Later, the brain was extracted and stored in 10% formalin for further histological analysis. Before histology, the brain was dipped in 30% sucrose solution at room temperature for about a day or two. Sectioning was done by taking 40 μm coronal brain sections using a cryostat (Thermo Fisher Scientific, USA) and mounted on the subbed glass slides. The sections were then stained with 0.1% cresyl violet, and the injection site was identified under a microscope and demonstrated in a reconstruction diagram (Figs. 1, 4, and 7).

Data analysis

The polysomnographic records were scored offline using "Somnologica Science Software" (Medcare Flaga, Iceland). Sleep recordings were manually scored using a four-second epoch length, employing the standard criteria for the rats⁴⁰. Low voltage and high-frequency EEG waves associated with increased motor activity were marked as wake; high voltage, low-frequency EEG waves (0.5–4 Hz) and decreased motor activity were marked as NREM sleep and low voltage, high-frequency EEG waves with a prominent theta peak (5–9 Hz) and nuchal muscle atonia were marked as REM sleep. The total time spent in the wake, NREM, and REM sleep was calculated. These values were expressed as percent amounts from hourly and mean values for the total recording time. The differences in the vigilant states after drug and vehicle microinjections were compared statistically with the baseline and vehicle values by one-way RM-ANOVA followed by the Tukey post hoc test.

Results

Effects of BaCl_2 microinjections in the LC on sleep–wake architecture

Microinjections of potassium inward rectifier channel inhibitor, BaCl_2 in the LC (Fig. 1), $n = 7$) significantly increased wakefulness ($p < 0.001$, $F_{(3,27)} = 31.02$) and decreased NREM sleep ($p < 0.001$, $F_{(3,27)} = 22.25$), as well as REM sleep ($p < 0.001$, $F_{(3,27)} = 152.84$) (one-way RM-ANOVA followed by Tukey post hoc) (Fig. 2A–C). The sites of microinjections of BaCl_2 in 7 animals were within LC, and 2 animals were located outside the LC (Fig. 1) (see Supplementary results). Microinjection of BaCl_2 outside the LC did not change wake, NREM sleep, and REM sleep amount (see Supplementary results and Fig. S1).

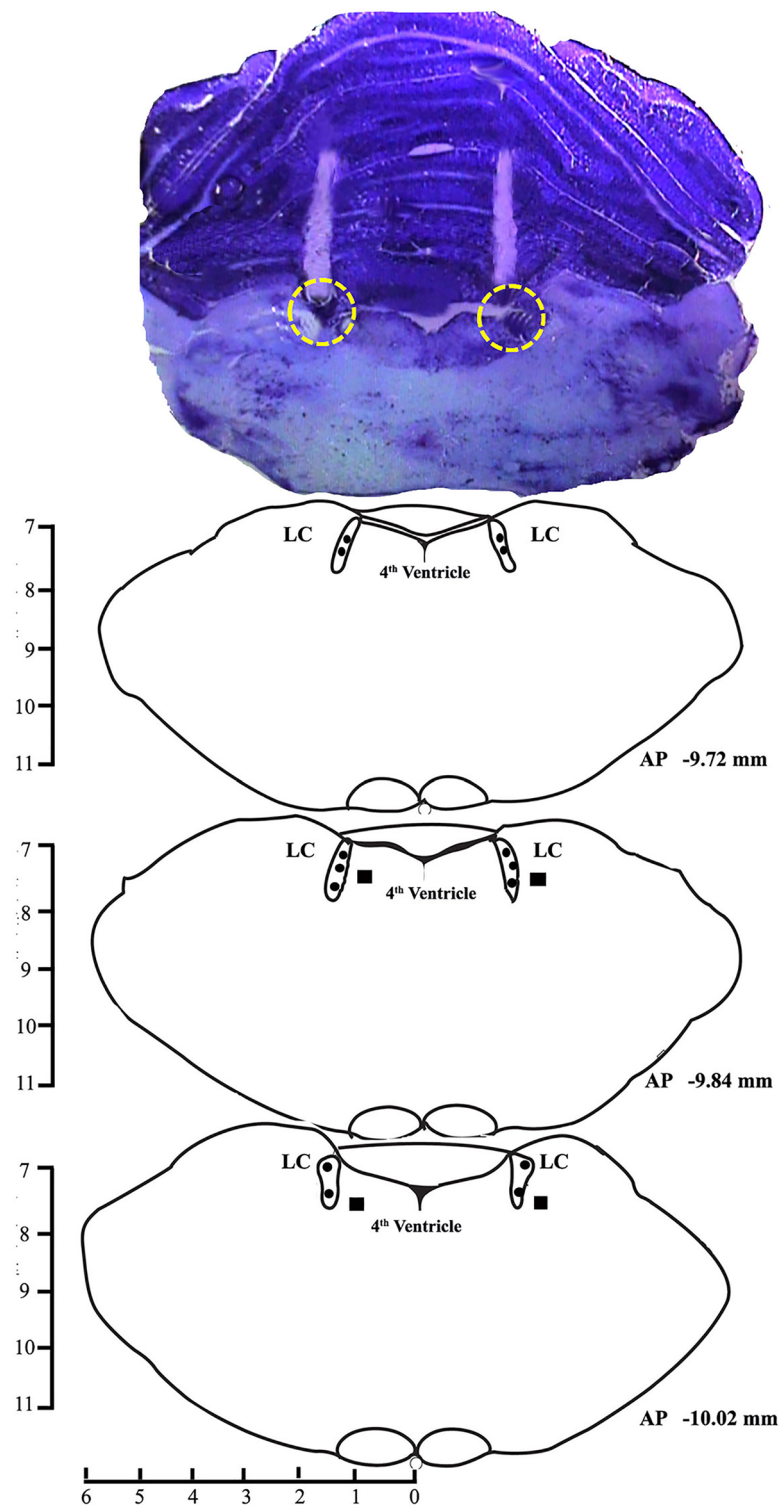


Fig. 1. A photomicrograph of 40 μm cresyl violet stained section and reconstruction diagram showing cannula tract and injection sites in the LC. Filled circles (\bullet) in the reconstruction diagram denote the site of injections within the LC and filled boxes (\blacksquare) denote the site of injections outside the LC.

The low dose of BaCl_2 (1 mM) increased wakefulness by 38% compared to baseline (Tukey, $p < 0.001$) and 40% compared to vehicle (Tukey, $p < 0.001$), respectively. Microinjection of a high dose of BaCl_2 (2 mM) significantly increased the amount of wakefulness by 54.6% compared to baseline (Tukey, $p < 0.001$) and 56.5% compared to vehicle (Tukey, $p < 0.001$), respectively (Fig. 2A).

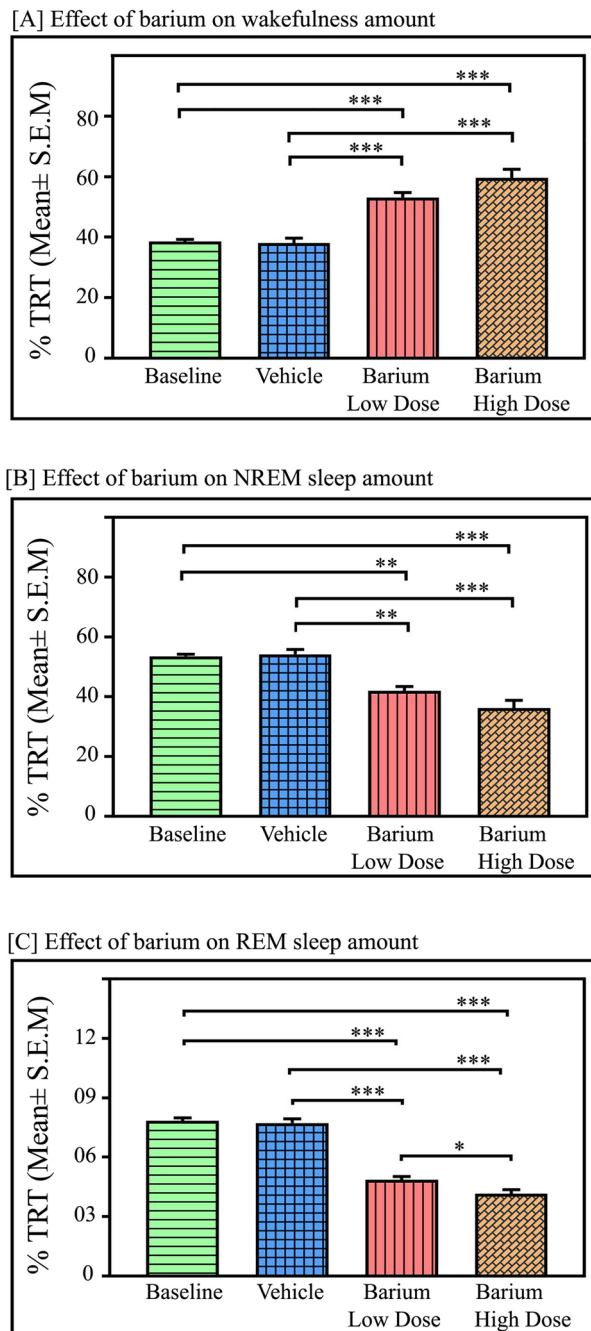


Fig. 2. Effects of Kir channel inhibition in the LC on sleep–wake architecture. Microinjections of Kir channel blocker BaCl₂ in the LC (n=7) significantly augmented wake and reduced NREM and REM sleep amounts. Microinjections at a low dose (1 mM) and high dose (2 mM) of BaCl₂ in the LC significantly increased (A) wakefulness ($p < 0.001$; $F_{(3,27)} = 31.02$), One-way RM ANOVA followed by Tukey post-hoc test. (B) Kir inhibition in LC significantly decreased NREM sleep ($p < 0.001$, $F_{(3,27)} = 22.25$). (C) Kir inhibition in LC significantly decreased REM sleep ($p < 0.001$, $F_{(3,27)} = 152.84$) (One Way RM ANOVA followed by Tukey post hoc test). * denotes $p < 0.05$, ** denotes $p < 0.01$, *** denotes $p < 0.001$.

In contrast, microinjections of BaCl₂ in the LC significantly decreased the NREM sleep amount ($p < 0.001$, $F_{(3,27)} = 22.25$) (one-way RM-ANOVA followed by Tukey post-hoc (Fig. 2B)). The low dose of BaCl₂ decreased NREM sleep by 22% compared to baseline (Tukey, $p < 0.01$) and 23% compared to vehicle (Tukey, $p < 0.01$). Whereas a high dose of BaCl₂ (2 mM) significantly decreased NREM sleep by 32.4% compared to baseline (Tukey, $p < 0.001$) and 33.2% compared to vehicle (Tukey, $p < 0.001$) (Fig. 2B).

Additionally, microinjections of BaCl₂ in the LC significantly decreased the amount of REM sleep in a dose-dependent manner [$p < 0.001$, $F_{(3,27)} = 152.84$] (one-way RM-ANOVA followed by Tukey post-hoc Fig. 2C)].

The low dose of BaCl₂ decreased REM sleep by 38% compared to baseline, (Tukey $p < 0.001$) and 37% compared to vehicle, (Tukey, $p < 0.001$). Whereas a high dose of BaCl₂ (2 mM) significantly decreased REM sleep by 47% compared to baseline (Tukey, $p < 0.001$) and 46% compared to vehicle (Tukey, $p < 0.001$) (Fig. 2C). Furthermore, a low dose of BaCl₂ (1 mM) decreased REM sleep amount by 15% compared to the high dose of BaCl₂ (2 mM) microinjections ($p < 0.05$), (one-way RM-ANOVA followed by Tukey post-hoc (Fig. 2C). Moreover, microinjection of both low and high doses of BaCl₂ in the LC significantly reduced the number of REM sleep episodes compared to the baseline and vehicle ($p < 0.001$, $F_{(3,27)} = 28.83$) (one-way RM-ANOVA followed by Tukey post-hoc) [Fig. 3A]. The low dose of BaCl₂ decreased the number of REM sleep episodes by 52.4% compared to baseline (Tukey, $p < 0.001$) and 54% compared to vehicle (Tukey, $p < 0.001$). Whereas a high dose of BaCl₂ (2 mM) significantly decreased the number of REM sleep episodes by 61% compared to baseline (Tukey, $p < 0.001$) and 63% compared to vehicle (Tukey, $p < 0.001$) (Fig. 3A). However, the length of REM sleep episodes did not change with low or high doses of BaCl₂ microinjections into the LC (Fig. 3B). Additionally, both low and high doses of BaCl₂ microinjections into the LC significantly increased the mean latency of REM sleep ($p < 0.001$, $F_{(3,27)} = 51.08$) (one-way RM-ANOVA followed by Tukey post-hoc (Fig. 3C). The low dose of BaCl₂ increased the mean latency of REM sleep by 28% compared to baseline (Tukey, $p < 0.01$) and 34% compared to vehicle (Tukey, $p < 0.01$). Whereas a high dose of BaCl₂ (2 mM) significantly increased the mean latency of REM sleep by 74% compared to baseline (Tukey, $p < 0.001$) and 82% compared to vehicle (Tukey, $p < 0.001$) (Fig. 3C).

Effects of BaCl₂ microinjections in the NTS on sleep–wake

Microinjections of potassium inward rectifier channel inhibitor BaCl₂ into the NTS (Fig. 4, $n = 7$) significantly decreased wakefulness ($p < 0.001$, $F_{(3,27)} = 91.26$). However, NREM sleep ($p < 0.001$, $F_{(3,27)} = 58.92$), as well as REM sleep ($p < 0.001$, $F_{(3,27)} = 183.70$) significantly increased (one-way RM-ANOVA followed by Tukey post hoc, Fig. 5A–C). The low dose of BaCl₂ (1 mM) decreased wakefulness by 29% compared to baseline (Tukey, $p < 0.001$) and 28% compared to vehicle (Tukey, $p < 0.001$), respectively. Whereas microinjection of a high dose of BaCl₂ (2 mM) significantly decreased the amount of wakefulness by 42% compared to baseline (Tukey, $p < 0.001$) and 41% compared to vehicle (Tukey, $p < 0.001$), respectively (Fig. 5A). Additionally, a high dose of BaCl₂ (2 mM) decreased wakefulness by 18% compared to a low dose of BaCl₂ in a dose-dependent manner (Tukey, $p < 0.01$) (Fig. 5A).

However, in contrast to the LC, microinjections of BaCl₂ in the NTS significantly increased NREM sleep ($p < 0.001$, $F_{(3,27)} = 58.92$), (one-way RM-ANOVA followed by Tukey post-hoc (Fig. 5B). The low dose of BaCl₂ increased NREM sleep by 19% compared to baseline (Tukey, $p < 0.001$) and 17% compared to vehicle (Tukey, $p < 0.001$). Whereas a high dose of BaCl₂ (2 mM) significantly increased NREM sleep by 26% compared to baseline (Tukey, $p < 0.001$) and 24.2% compared to vehicle (Tukey, $p < 0.001$) (Fig. 5B).

Interestingly, microinjections of BaCl₂ in the NTS significantly augmented REM sleep amount in a dose-dependent manner ($p < 0.001$, $F_{(3,27)} = 183.70$) (one-way RM-ANOVA followed by Tukey post-hoc (Fig. 5C). The low dose of BaCl₂ increased REM sleep by 29.4% compared to baseline (Tukey, $p < 0.001$) and 30.5% compared to vehicle (Tukey, $p < 0.001$). Whereas a high dose of BaCl₂ (2 mM) significantly increased REM sleep by 44% compared to baseline (Tukey, $p < 0.001$) and 45% compared to vehicle (Tukey, $p < 0.001$) (Fig. 5C). Moreover, a high dose of BaCl₂ (2 mM) significantly increased REM sleep amount by 12% compared to a low dose (Tukey, $p < 0.01$) in a dose-dependent manner. Additionally, microinjection of both low and high doses of BaCl₂ into the NTS significantly increased the mean number of REM sleep episodes compared to the baseline and vehicle ($p < 0.001$, $F_{(3,27)} = 9.54$) (one-way RM-ANOVA followed by Tukey post-hoc (Fig. 6A). The low dose of BaCl₂ increased the number of REM sleep episodes by 44% compared to baseline (Tukey, $p < 0.05$) and 42.5% compared to vehicle (Tukey, $p < 0.05$). Whereas a high dose of BaCl₂ (2 mM) significantly increased the number of REM sleep episodes by 57% compared to baseline (Tukey, $p < 0.01$) and 55.7% compared to vehicle (Tukey, $p < 0.01$) (Fig. 6A). However, both doses of the BaCl₂ microinjections into the NTS did not change REM sleep episode length (Fig. 6B), suggesting that Kir channel inhibition in the NTS enhances REM sleep primarily by transiting REM sleep episode numbers from NREM sleep.

Additionally, both low and high doses of BaCl₂ microinjections into the NTS significantly decreased the mean latency of REM sleep ($p < 0.001$, $F_{(3,27)} = 39.80$) (one-way RM-ANOVA followed by Tukey post-hoc (Fig. 6C). The low dose of BaCl₂ decreased the mean latency of REM sleep by 35.5% compared to baseline (Tukey, $p < 0.001$) and 31.3% compared to vehicle (Tukey, $p < 0.001$). Whereas a high dose of BaCl₂ (2 mM) significantly decreased the mean latency of REM sleep by 48% compared to baseline (Tukey, $p < 0.001$) and 45% compared to vehicle (Tukey, $p < 0.001$) (Fig. 6C).

Effects of BaCl₂ microinjections in the RTN on sleep–wake architecture

We next investigated if Kir channel inhibition in RTN neurons also modulates sleep–wake since it has been reported that both neurons and astrocytes of RTN express Kir channels abundantly. Microinjections of potassium inward rectifier channel inhibitor, BaCl₂, into the RTN (Fig. 7, $n = 6$) significantly increased wakefulness ($p < 0.001$, $F_{(3,23)} = 78.85$). However, NREM sleep significantly decreased ($p < 0.001$, $F_{(3,23)} = 88.61$) (one-way RM-ANOVA followed by Tukey post-hoc) (Fig. 8). We did not find any significant change in REM sleep amount after microinjections of either low or high dose of BaCl₂ in the RTN (Fig. 8C). The low dose of BaCl₂ microinjection (1 mM) increased wakefulness by 29% compared to baseline (Tukey, $p < 0.001$) and 27% compared to vehicle (Tukey, $p < 0.001$), respectively (Fig. 8A). Microinjection of high dose of BaCl₂ (2 mM) significantly increased the amount of wakefulness by 41% compared to baseline, (Tukey, $p < 0.01$) and 38% compared to vehicle, (Tukey, $p < 0.01$), respectively (Fig. 8A). Further, a high dose of BaCl₂ microinjections into the RTN increased the amount of wakefulness by 10% compared to the low dose (Tukey, $p < 0.05$) (Fig. 8A). The sites of microinjections of BaCl₂

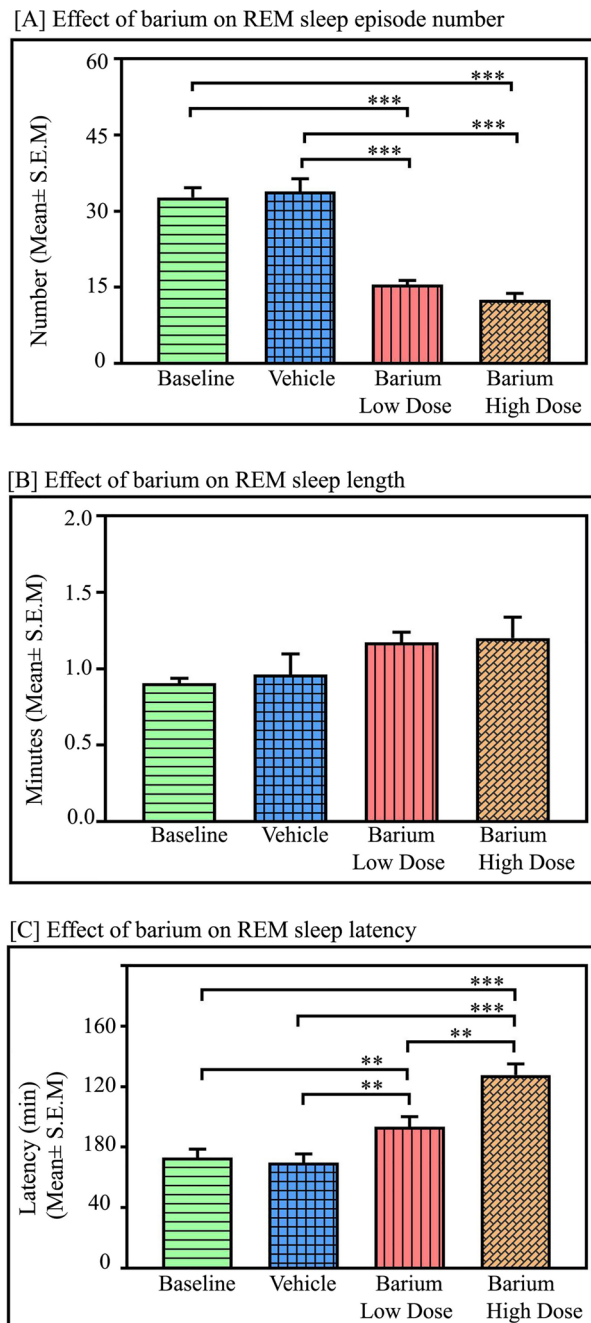


Fig. 3. Effects of Kir channel inhibition in the LC on REM sleep parameters: Effects of Kir channel inhibition in the LC on REM sleep parameters. **(A)** Microinjections of low and high doses of BaCl₂ (n=7) in the LC significantly decreased the mean number of REM sleep episodes in contrast to the baseline and vehicle ($p < 0.001$, $F_{(3,27)} = 28.83$), (one-way RM-ANOVA followed by Tukey post-hoc test). **(B)** However, REM sleep episode length did not change with low dose or high dose of BaCl₂ microinjections into the LC when compared to the vehicle ($p > 0.05$, $F_{(3,27)} = 68.38$). **(C)** REM sleep latency was significantly increased after microinjections of low and high doses of BaCl₂ into the LC ($p < 0.001$, $F_{(3,27)} = 51.08$) (one-way RM-ANOVA followed by Tukey post-hoc test). ** denotes $p < 0.01$, *** denotes $p < 0.001$.

in 6 animals were within RTN, and 2 animals were outside the RTN (Fig. 7). Microinjection of BaCl₂ outside the RTN did not change wake, NREM sleep, and REM sleep amount (see Supplementary results and Fig. S2).

Microinjection of BaCl₂ in the RTN significantly decreased the amount of NREM sleep ($p < 0.001$, $F_{(3,23)} = 88.61$), (one-way RM-ANOVA followed by Tukey post hoc, Fig. 8B). The low dose of BaCl₂ decreased NREM sleep by 20% compared to baseline, (Tukey, $p < 0.001$) and 19% compared to vehicle, (Tukey, $p < 0.001$). Whereas a high dose of BaCl₂ (2 mM) significantly decreased NREM sleep by 28% compared to baseline (Tukey, $p < 0.001$) and 26.5% compared to vehicle (Tukey, $p < 0.001$) (Fig. 8B). Additionally, a high dose of BaCl₂

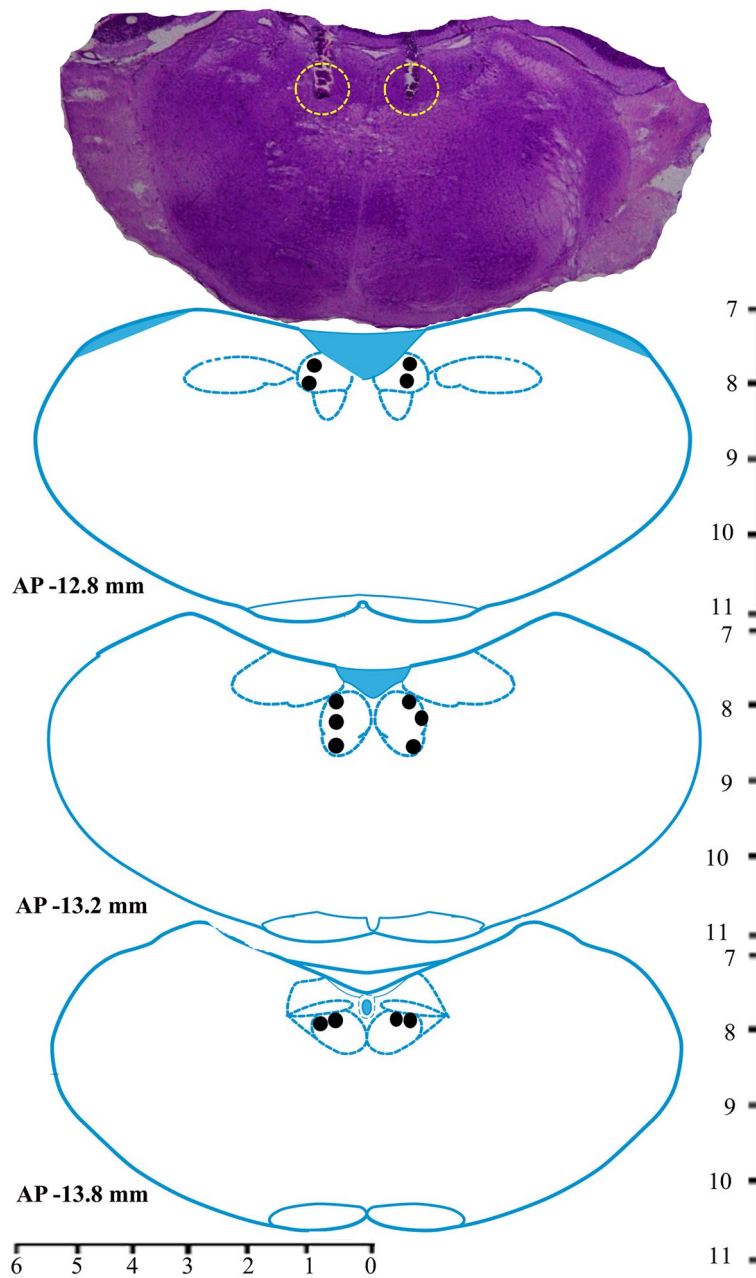


Fig. 4. A photomicrograph of 40 μm cresyl violet stained section and reconstruction diagram showing cannula tract and injection sites in the NTS. Filled circles (\bullet) in the reconstruction diagram denote the site of injections within the NTS.

microinjections into the RTN decreased the amount of NREM sleep by 10% compared to the low dose (Tukey, $p < 0.01$) (Fig. 8B). However, microinjections of BaCl_2 in the RTN did not significantly change the amount of REM sleep compared to the baseline and vehicle groups (Fig. 8C).

Discussion

Our results show differential effects of Kir channel inhibition in the LC, NTS, and RTN on sleep–wake architecture. In the LC and RTN, inhibition of Kir channels led to an increased wakefulness and decreased NREM sleep. Conversely, inhibition of Kir channels in the NTS resulted in decreased wakefulness and increased NREM and REM sleep. Inhibiting Kir channels in the LC led to a significant reduction in REM sleep, while similar inhibition in the RTN did not produce notable changes in REM sleep. Interestingly, inhibiting Kir channels in the NTS increased REM sleep, primarily due to higher frequency of REM sleep episodes and a shorter latency to REM sleep. It can be surmised that the Kir channels in the NTS may play a crucial role in initiating REM sleep rather than its maintenance. Similar results were not observed when BaCl_2 was microinjected outside the LC and RTN

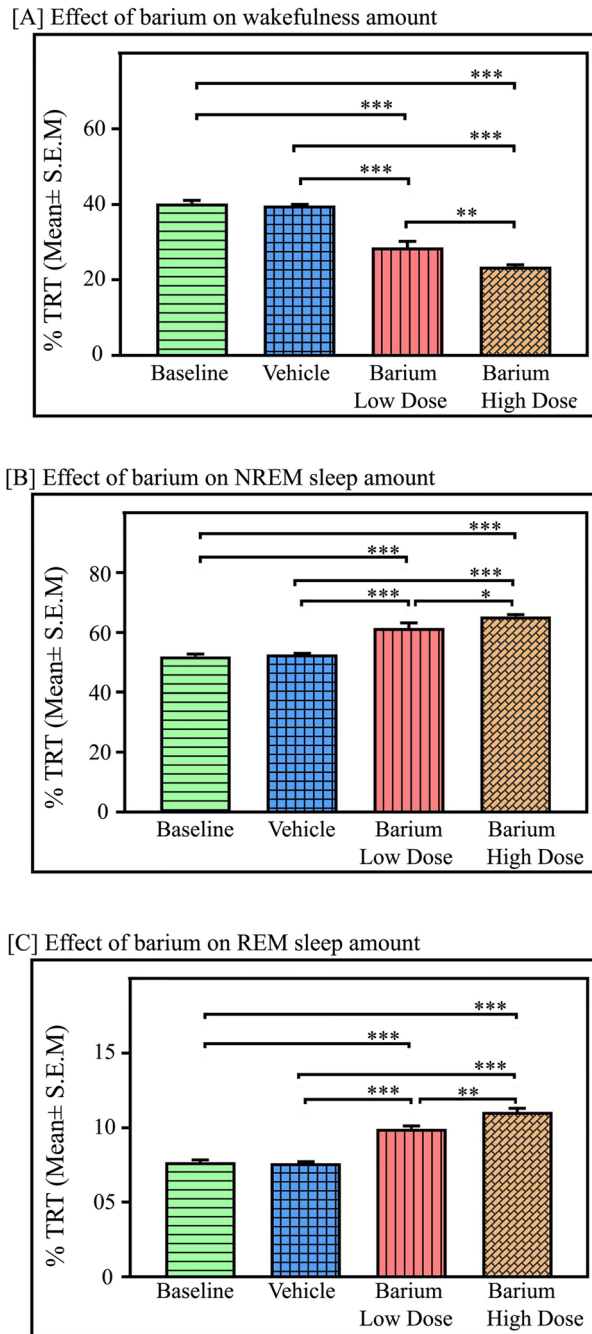


Fig. 5. Effects of Kir channel inhibition in the NTS on sleep–wake architecture. Microinjections of Kir channel blocker BaCl₂ in the NTS (n = 7) significantly decreased the percent amount of wake but increased NREM and REM sleep. **(A)** Microinjections of low dose (1 mM) and high dose (2 mM) of BaCl₂ in the NTS significantly decreased wakefulness ($p < 0.001$, $F_{(3,27)} = 91.26$), compared to the baseline and vehicle microinjections. **(B)** However, compared to baseline and vehicle, both the dose of BaCl₂ microinjections into the NTS significantly augmented NREM sleep amount ($p < 0.001$, $F_{(3,27)} = 58.92$), **(C)** Further, microinjections of low as well as high doses of BaCl₂ into the NTS significantly increased REM sleep amount in a dose-dependent manner ($p < 0.001$, $F_{(3,27)} = 183.70$, one-way RM-ANOVA followed by Tukey post hoc test). ** denotes $p < 0.01$, *** denotes $p < 0.001$.

(Supplementary results). These findings indicate that Kir channels in the LC, RTN, and NTS chemosensory regions affect sleep–wake patterns. Additionally, they suggest that Kir channels in the NTS, but not in the LC or RTN, regulate the transition from NREM to REM sleep.

The Kir channels are the potential central CO₂/H⁺ sensor⁴¹. When CO₂/H⁺ is detected, the inhibition of K⁺ current plays a critical role in chemosensory neuronal membrane depolarization and subsequent processes like Ca²⁺ influx and neurotransmitter release^{41,42}. Kir channels are inhibited when the surrounding pH is decreased⁴³.

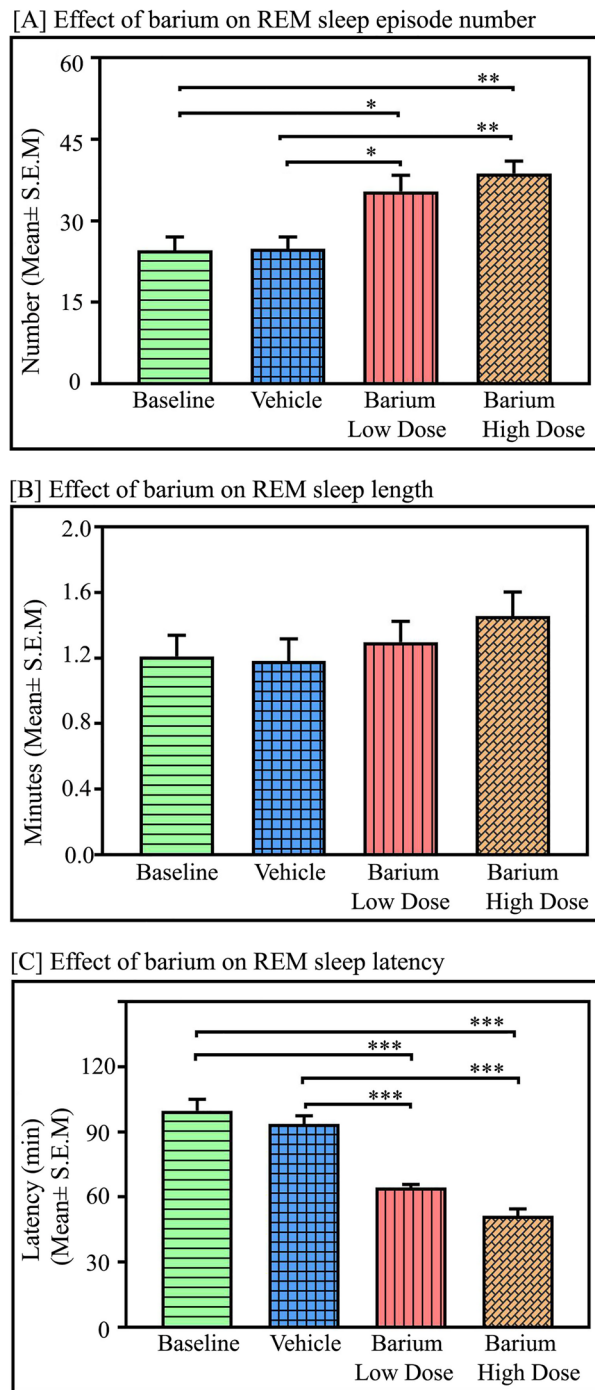


Fig. 6. Effects of Kir channel inhibition in the NTS on REM sleep parameters. Microinjections of kir channel blocker BaCl_2 in the NTS ($n=7$) significantly increased (A) the average number of REM sleep episodes ($p < 0.001$, $F_{(3,27)} = 9.54$) but we did not observe any significant change in REM sleep episode length (B). However, kir channel inhibition in the NTS by low as well as high doses of BaCl_2 significantly decreased the average latency of REM sleep episodes ($p < 0.001$, $F_{(3,27)} = 39.80$, One-way RM-ANOVA followed by Tukey post-hoc test). *Denotes $p < 0.05$, ** denotes $p < 0.01$, *** denotes $p < 0.001$.

The conductance through Kir channels in the LC neurons is reduced in response to hypercapnic acidosis⁴³. Furthermore, hypoxia and normoxic-hypercapnia-mediated changes in ventilatory responses are totally abolished in Kir5.1 knockout mice⁴⁴. Conversely, Ca^{2+} -activated K^+ channels are inhibited during hypercapnic hypoxia⁴⁵. These findings suggest that Kir channels in the chemosensitive neurons are crucial in detecting hypercapnic acidosis^{43,46}. Additionally, Kir channel conductance increases with hyperpolarization, and the closure of these channels at depolarized potentials permits more prolonged action potentials⁴⁷. Therefore, adjusting Kir channel

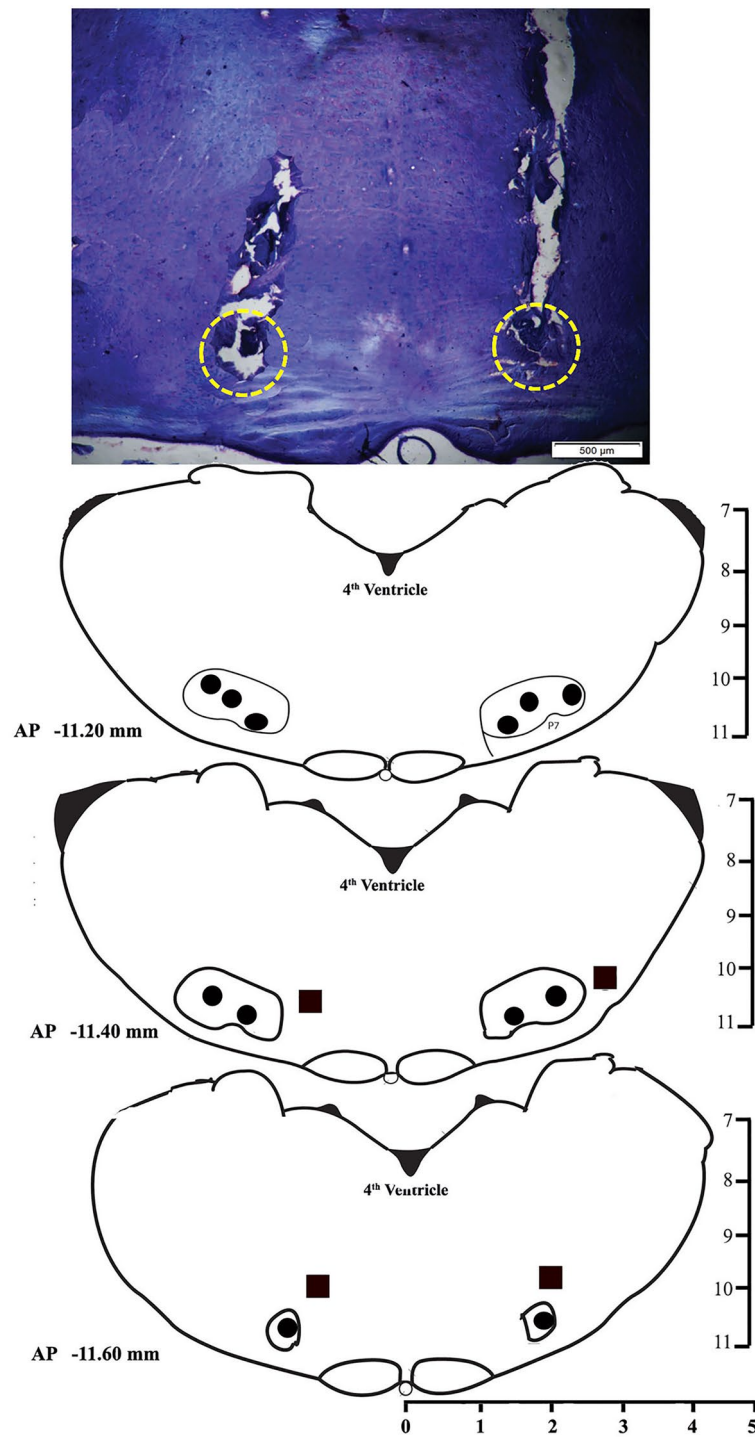


Fig. 7. A photomicrograph of 40 μm cresyl violet stained section and reconstruction diagram showing cannula tract and injection sites in the RTN. Filled circles (\bullet) in the reconstruction diagram denote the site of injections within the RTN, and filled boxes (\blacksquare) denote the site of injections outside of the RTN.

conductance can effectively regulate a neuron's membrane potential and neuronal excitability⁴⁷. These studies suggest that Kir channels regulate ionic homeostasis at the membrane of various neurons and are also involved in H^+ sensing processes and central chemoregulation.

Fluctuations in bodily pH/ CO_2 levels, resulting from different physiological and environmental factors, can alter the overall sleep–wake architecture. Alteration in bodily pH after meal, respiratory disorders like sleep apnea, central hypoventilation syndrome, and moderately increased CO_2 levels inside the room alter sleep–wake architecture profoundly^{7,48–50}. Similarly, moderate hypercapnia induced by infusion of 2–4% CO_2 in breathing air

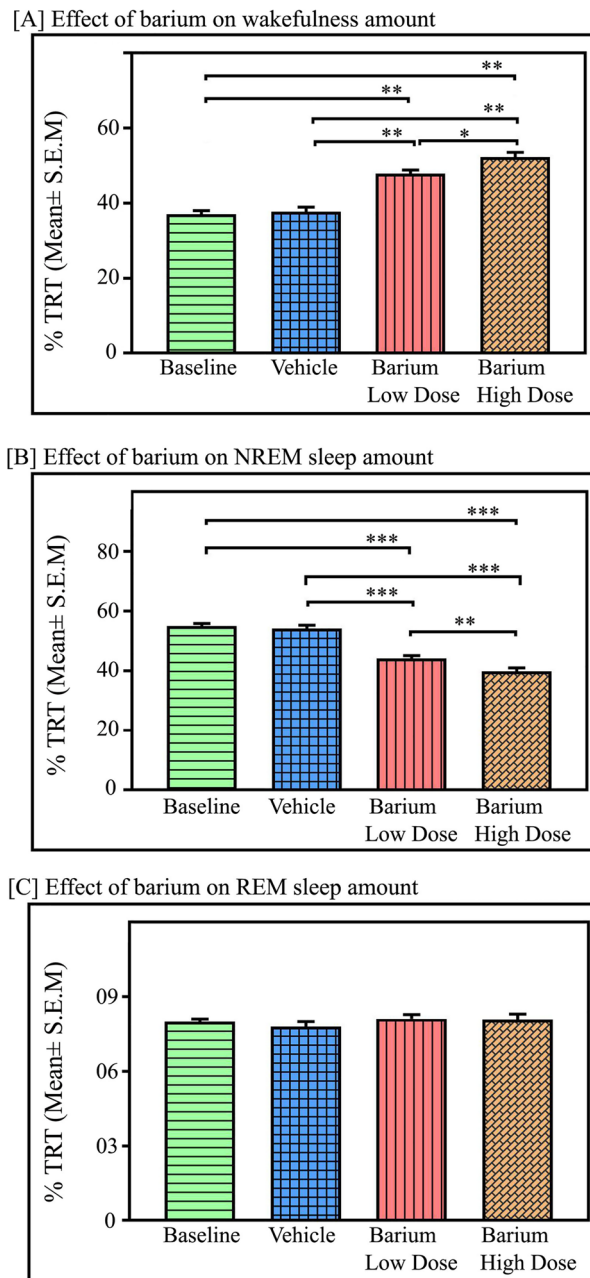


Fig. 8. Effects of Kir channel inhibition in the RTN on sleep-wake architecture. Microinjections of kir channel blocker BaCl_2 in the RTN ($n=6$) significantly increased (A) wakefulness amount compared to the baseline and vehicle ($p < 0.01$, $F_{(3,23)} = 78.85$), One way RM ANOVA, followed by post-hoc Tukey test. (B) However, BaCl_2 microinjections with low dose (1 mM) and high dose (2 mM) in the RTN significantly decreased NREM sleep amount compared to baseline and vehicle ($p < 0.001$, $F_{(3,23)} = 88.61$). (C) However, REM sleep amount did not change either with a low dose or a high dose of BaCl_2 microinjections into the RTN compared to baseline or vehicle ($p > 0.05$; $F_{(3,23)} = 40.39$). *Denotes $p < 0.05$, ** denotes $p < 0.01$, *** denotes $p < 0.001$.

increases NREM sleep amount and REM sleep episode numbers^{11,33,51}. Studies suggest that during NREM sleep, reduced breathing rates lead to a rise in bodily CO_2 levels, which are then regulated back to normal through increased breathing^{7,9}. Consequently, it is plausible that the accumulation of CO_2 within a narrow range during NREM sleep could facilitate the transition into REM sleep to help expel excess CO_2 without disrupting sleep^{1,7}. However, if the CO_2 is accumulated to a greater extent, it may cause either micro or macro arousal^{1,11,34}. The execution of such a shift from NREM to REM sleep under increased CO_2 levels unquestionably depends on the function of chemosensory machinery in the brainstem. Our recent findings are consistent with this supposition that chemosensory neurons in the LC, with the help of proton pumps and acid-sensing ion channels, help initiate the transition from NREM to REM sleep under normocapnic as well as hypercapnic conditions¹¹.

The brainstem's chemosensory machinery possibly play dualistic and complementary functions^{11,23,52}. For example, the LC is one of the essential chemosensory areas with a well-established role as one of the wake-centers in the brain. Its neuronal activation causes arousal and inhibition or lesion promotes sleep^{28,29,53,54}. Similarly, the NTS has dual functional chemoregulatory and sleep-promoting circuitries^{14,20,31,32}. Studies suggest that high-frequency electrical stimulation of NTS induces REM sleep¹³. A group of neurons in the NTS exhibits an increased firing rate during NREM sleep, and possibly endogenous opioid receptors contribute to NREM sleep induction^{32,55}. For the RTN, studies suggest that optogenetic stimulation of these neurons triggers sleep-dependent cardio-respiratory changes that ultimately lead to arousal from sleep^{12,27}. Furthermore, the RTN acidification or optogenetic activation causes arousal and increased breathing during wake and NREM sleep but not during REM sleep, suggesting that the RTN also plays an essential role in NREM sleep-dependent breathing drive⁵⁶. It is, however, not clear why different chemosensory brain areas influence S–W differently, but it can be attributed to their optimal capacity to sense the changes in pH. The sensitivity of neurons in these three areas to pH changes varies significantly. A narrow range of pH changes activates some neurons, while others only respond to substantial pH reductions, indicating they are sensitive to a broader pH range⁵⁷. Therefore, it is likely that shifts in vigilance states from NREM sleep to wakefulness or REM sleep might be driven by excessive or minute alterations in pH levels respectively. For example, a major alteration in the pH level would induce wake, while mild hypercapnia would induce REM sleep. The neural system cannot sustain a prolonged hypercapnic state during NREM sleep. It must rapidly be corrected by increasing the breathing rate, which occurs during either wakefulness or REM sleep. Frequent awakenings from NREM sleep are not typical of normal physiology, as they can result in medical conditions like sleep apnea. Hence, it has been proposed that one of the functions of REM sleep is to maintain a normal brain CO₂ level for sustained and unperturbed sleep⁷.

This study further enhances our understanding of the role of Kir channels in the brainstem's chemosensory system and its integration with the regulation of sleep–wake cycles. Previously, studies have reported that kir channels on cranial motor neurons regulate genioglossal muscle activity, thereby regulating breathing during REM sleep^{57,58}. Further studies have also reinforced the role of Kir channels in the pCO₂/pH-dependent modulation of cardiovascular and respiratory physiology⁵⁹. Kir channels also play a role in the pathophysiology of obstructive sleep apnea. Kir gene expression has shown a significant correlation with the severity of sleep apnea, suggesting their involvement in apneic events⁶⁰. Additionally, the increase in circulating Kir proteins following positive airway pressure therapy further implies their role in obstructive sleep apnea⁶⁰. Interestingly, sleep apnea is associated with sleep fragmentation and repeated arousals from sleep, which pose a greater risk for the development of cardio-respiratory diseases as well as cognitive impairments^{9,61}. On the other hand, studies suggest that sleep and anesthesia drastically reduced cortical extracellular levels of K⁺ ions, and extracellular application of K⁺ by micro-iontophoresis causes arousal from sleep, implying that K⁺-dependent sleep-state transitions occur quickly⁶². It is interesting to note that during sleep, extracellular K⁺ levels decrease; however, the underlying mechanism is not known. Kir channels are inward-rectifiers that move K⁺ inside more swiftly than outside; hence, they could be involved in vigilance state-dependent K⁺ homeostatic balance. All these studies suggest that kir channels in the brainstem may be involved in the sleep-to-wake transition. This study expands our understanding by showing that Kir channels in the NTS, but not in the LC and RTN, influence the transition from NREM to REM sleep.

In conclusion, our study provides insights into the role of chemosensory machinery in regulating state transitions from NREM sleep to REM sleep/wakefulness during the sleep time of the circadian phase. This mechanism is crucial to a 'brainstem alarm' executive circuit that may govern state transition responses mediated by hypercapnia, such as (i) abrupt changes in pH can trigger wakefulness from NREM sleep, and (ii) mild changes in pH can induce REM sleep from NREM sleep. The dynamic transition from NREM to REM sleep may restore H⁺ homeostasis by increasing breathing rates to expel excessive CO₂. This transition helps prevent repeated arousals from sleep, which pose significant risks to cardiovascular and respiratory health and cognitive function⁶³. Further, chemosensory dysfunctions may contribute to various sleep-related breathing disorders, such as sleep apnea, congenital central hypoventilation syndrome, sudden infant death syndrome, etc. Future studies should identify specific subsets of neurons within central chemosensory areas that play dualistic roles in regulating the initiation or termination of sleep states based on bodily CO₂ levels and other ionic disturbances. Such findings hold promise for developing novel treatment strategies and management approaches for various sleep-related breathing disorders.

Data availability

All the data used in the current study will be available from the corresponding and co-author upon reasonable request.

Received: 28 May 2024; Accepted: 30 August 2024

Published online: 17 September 2024

References

1. Mir, F. A., Jha, S. K. & Jha, V. M. The role of sleep in homeostatic regulation of ionic balances and its implication in cognitive functions. In *Sleep, Memory and Synaptic Plasticity*. (eds Jha, S. & Jha, V.) 77–106. https://doi.org/10.1007/978-981-13-2814-5_4 (Springer Singapore, 2019).
2. Jha, S. K., Brennan, F. X., Pawlyk, A. C., Ross, R. J. & Morrison, A. R. REM sleep: A sensitive index of fear conditioning in rats. *Eur. J. Neurosci.* **21**, 1077–1080. <https://doi.org/10.1111/j.1460-9568.2005.03920.x> (2005).
3. Song, C. & Tagliazucchi, E. Linking the nature and functions of sleep: Insights from multimodal imaging of the sleeping brain. *Curr. Opin. Physiol.* **15**, 29–36. <https://doi.org/10.1016/j.cophys.2019.11.012> (2020).
4. Girardeau, G. & Lopes-dos-Santos, V. Brain neural patterns and the memory function of sleep. *Science* **374**, 560–564. <https://doi.org/10.1126/science.abi8370> (2021).

5. Van Dort, C. J. Locus coeruleus neural fatigue: A potential mechanism for cognitive impairment during sleep deprivation. *Sleep* **39**, 11–12. <https://doi.org/10.5665/sleep.5302> (2016).
6. Jha, V. M. & Jha, S. K. *Sleep: Evolutionary and Adaptive Changes in Birds and Mammals* (Springer, Singapore, 2020).
7. Madan, V. & Jha, S. K. A moderate increase of physiological CO₂ in a critical range during stable NREM sleep episode: A potential gateway to REM sleep. *Front. Neurol.* **3**, 19 (2012).
8. Penzel, T., Kantelhardt, J. W., Lo, C. C., Voigt, K. & Vogelmeier, C. Dynamics of heart rate and sleep stages in normals and patients with sleep apnea. *Neuropsychopharmacology* **28**(Suppl 1), S48–S53. <https://doi.org/10.1038/sj.npp.1300146> (2003).
9. McKay, L., Atalla, A. & Morrell, M. Physiology and neural control of breathing during sleep. In *Sleep Apnoea. Series: European Respiratory Society Monograph Series* (50). (eds McNicholas, W.T. & Bonsignore, M.R.) 1–16. <https://doi.org/10.1183/1025448x.00023909> (European Respiratory Society, 2010).
10. Nagai, M., Hoshida, S. & Kario, K. Sleep duration as a risk factor for cardiovascular disease—a review of the recent literature. *Curr. Cardiol. Rev.* **6**, 54–61. <https://doi.org/10.2174/157340310790231635> (2010).
11. Mir, F. A. & Jha, S. K. Proton pump inhibitor “Lansoprazole” inhibits locus coeruleus’s neuronal activity and increases rapid eye movement sleep. *ACS Chem. Neurosci.* **12**, 4265–4274. <https://doi.org/10.1021/acscchemneuro.1c00185> (2021).
12. Guyenet, P. G., Stornetta, R. L., Abbott, S. B. G., Depuy, S. D. & Kanbar, R. The retrotrapezoid nucleus and breathing. *Adv. Exp. Med. Biol.* **758**, 115–122. https://doi.org/10.1007/978-94-007-4584-1_16 (2012).
13. Martínez-Vargas, D., Valdés-Cruz, A., Magdaleno-Madrigal, V. M., Fernández-Mas, R. & Almazán-Alvarado, S. Effect of electrical stimulation of the nucleus of the solitary tract on electroencephalographic spectral power and the sleep-wake cycle in freely moving cats. *Brain Stimul.* **10**, 116–125. <https://doi.org/10.1016/j.brs.2016.08.012> (2017).
14. Coates, E. L., Li, A. & Nattie, E. E. Widespread sites of brain stem ventilatory chemoreceptors. *J. Appl. Physiol.* **75**, 5–14. <https://doi.org/10.1152/jappl.1993.75.1.5> (1993).
15. Nattie, E. E. Central chemosensitivity, sleep, and wakefulness. *Respir. Physiol.* **129**, 257–268. [https://doi.org/10.1016/s0034-5687\(01\)00295-x](https://doi.org/10.1016/s0034-5687(01)00295-x) (2001).
16. Huda, R. *et al.* Acid-sensing ion channels contribute to chemosensitivity of breathing-related neurons of the nucleus of the solitary tract. *J. Physiol.* **590**, 4761–4775. <https://doi.org/10.1113/jphysiol.2012.232470> (2012).
17. Oyamada, Y., Ballantyne, D., Muckenhoff, K. & Scheid, P. Respiration-modulated membrane potential and chemosensitivity of locus coeruleus neurons in the in vitro brainstem-spinal cord of the neonatal rat. *J. Physiol.* **513**(Pt 2), 381–398. <https://doi.org/10.1111/j.1469-7793.1998.381bb.x> (1998).
18. Biancardi, V., Bicego, K. C., Almeida, M. C. & Gargaglioni, L. H. Locus coeruleus noradrenergic neurons and CO₂ drive to breathing. *Pflüg. Archiv-Eur. J. Physiol.* **455**, 1119–1128 (2008).
19. Fu, C. *et al.* Activation of Phox2b-expressing neurons in the nucleus tractus solitarii drives breathing in mice. *J. Neurosci.* **39**, 2837–2846. <https://doi.org/10.1523/jneurosci.2048-18.2018> (2019).
20. Cheng, Z., Guo, S. Z., Lipton, A. J. & Gozal, D. Domoic acid lesions in nucleus of the solitary tract: Time-dependent recovery of hypoxic ventilatory response and peripheral afferent axonal plasticity. *J. Neurosci.* **22**, 3215–3226. <https://doi.org/10.1523/jneurosci.22-08-03215.2002> (2002).
21. Fu, C. *et al.* Chemosensitive Phox2b-expressing neurons are crucial for hypercapnic ventilatory response in the nucleus tractus solitarius. *J. Physiol.* **595**, 4973–4989. <https://doi.org/10.1113/jp274437> (2017).
22. Akilesh, M. R., Kamper, M., Li, A. & Nattie, E. E. Effects of unilateral lesions of retrotrapezoid nucleus on breathing in awake rats. *J. Appl. Physiol.* **82**, 469–479. <https://doi.org/10.1152/jappl.1997.82.2.469> (1997).
23. Czeisler, C. M. *et al.* The role of PHOX2B-derived astrocytes in chemosensory control of breathing and sleep homeostasis. *J. Physiol.* **597**, 2225–2251. <https://doi.org/10.1113/jp277082> (2019).
24. Li, A., Emond, L. & Nattie, E. Brainstem catecholaminergic neurons modulate both respiratory and cardiovascular function. *Adv. Exp. Med. Biol.* **605**, 371–376. https://doi.org/10.1007/978-0-387-73693-8_65 (2008).
25. Aston-Jones, G. *et al.* Afferent regulation of locus coeruleus neurons: Anatomy, physiology and pharmacology. *Progr. Brain Res.* **88**, 47–75 (1991).
26. Jha, S. K. & Mallick, B. N. in *Rapid Eye Movement Sleep* (eds Birendra N Mallick, S. R. Pandi-Perumal, Robert W. McCarley, & Adrian R. Morrison) 173–182 (Cambridge University Press, 2011).
27. Abbott, S. B., Coates, M. B., Stornetta, R. L. & Guyenet, P. G. Optogenetic stimulation of c1 and retrotrapezoid nucleus neurons causes sleep state-dependent cardiorespiratory stimulation and arousal in rats. *Hypertension* **61**, 835–841. <https://doi.org/10.1161/hypertensionaha.111.00860> (2013).
28. Carter, M. E. *et al.* Tuning arousal with optogenetic modulation of locus coeruleus neurons. *Nat. Neurosci.* **13**, 1526–1533. <https://doi.org/10.1038/nn.2682> (2010).
29. Pirhajati Mahabadi, V. *et al.* Effects of bilateral lesion of the locus coeruleus on the sleep-wake cycle in the rat. *Physiol. Pharmacol.* **19**, 22–30 (2015).
30. Yamaguchi, H., Hopf, F. W., Li, S.-B. & de Lecea, L. In vivo cell type-specific CRISPR knockdown of dopamine beta hydroxylase reduces locus coeruleus evoked wakefulness. *Nat. Commun.* **9**, 5211. <https://doi.org/10.1038/s41467-018-07566-3> (2018).
31. Magness, J., Moruzzi, G. & Pompeiano, O. *Synchronization of the EEG produced by low-frequency electrical stimulation of the region of the solitary tract.* <https://search.worldcat.org/title/synchronization-of-the-ee-g-produced-by-low-frequency-electrical-stimulation-of-the-region-of-the-solitary-tract/oclc/467968239> (Air Force Office of Scientific Research, Air Research and Development Command, USAF, 1960).
32. Eguchi, K. & Satoh, T. Convergence of sleep-wakefulness subsystems onto single neurons in the region of cat’s solitary tract nucleus. *Archives Italiennes de Biologie* **118**, 331–345 (1980).
33. Fraigne, J. J., Dunin-Barkowski, W. L. & Orem, J. M. Effect of hypercapnia on sleep and breathing in unanesthetized cats. *Sleep* **31**, 1025–1033 (2008).
34. Mir, F. A. & Jha, S. K. Locus coeruleus acid-sensing ion channels modulate sleep-wakefulness and state transition from NREM to REM sleep in the rat. *Neurosci. Bull.* **37**, 684–700 (2021).
35. Wenker, I. C., Kréneisz, O., Nishiyama, A. & Mulkey, D. K. Astrocytes in the retrotrapezoid nucleus sense H⁺ by inhibition of a Kir4.1–Kir5.1-like current and may contribute to chemoreception by a purinergic mechanism. *J. Neurophysiol.* **104**, 3042–3052. <https://doi.org/10.1152/jn.00544.2010> (2010).
36. Chen, K., Zuo, D., Liu, Z. & Chen, H. Kir2.1 channels set two levels of resting membrane potential with inward rectification. *Pflug. Arch. Eur. J. Physiol.* **470**, 599–611. <https://doi.org/10.1007/s00424-017-2099-3> (2018).
37. Zhang, X. *et al.* The disruption of central CO₂ chemosensitivity in a mouse model of Rett syndrome. *Am. J. Physiol. Cell Physiol.* **301**, C729–C738. <https://doi.org/10.1152/ajpcell.00334.2010> (2011).
38. Wu, J., Xu, H., Shen, W. & Jiang, C. Expression and coexpression of CO₂-sensitive Kir channels in brainstem neurons of rats. *J. Membr. Biol.* **197**, 179–191. <https://doi.org/10.1007/s00232-004-0652-4> (2004).
39. Xu, H., Cui, N., Yang, Z., Qu, Z. & Jiang, C. Modulation of kir4.1 and kir5.1 by hypercapnia and intracellular acidosis. *J. Physiol.* **524**(Pt 3), 725–735. <https://doi.org/10.1111/j.1469-7793.2000.00725.x> (2000).
40. Jha, S. K. & Mallick, B. N. Presence of α -1 norepinephrine and GABA-A receptors on medial preoptic hypothalamus thermosensitive neurons and their role in integrating brainstem ascending reticular activating system inputs in thermoregulation in rats. *Neuroscience* **158**, 833–844. <https://doi.org/10.1016/j.neuroscience.2008.10.038> (2009).

41. Yamamoto, Y. *et al.* Immunohistochemical distribution of inwardly rectifying K⁺ channels in the medulla oblongata of the rat. *J. Vet. Med. Sci. Jpn. Soc. Vet. Sci.* **70**, 265–271. <https://doi.org/10.1292/jvms.70.265> (2008).
42. Lahiri, S. & Forster, R. E. CO₂/H⁺ sensing: Peripheral and central chemoreception. *Int. J. Biochem. Cell Biol.* **35**, 1413–1435. [https://doi.org/10.1016/S1357-2725\(03\)00050-5](https://doi.org/10.1016/S1357-2725(03)00050-5) (2003).
43. Pineda, J. & Aghajanian, G. K. Carbon dioxide regulates the tonic activity of locus coeruleus neurons by modulating a proton- and polyamine-sensitive inward rectifier potassium current. *Neuroscience* **77**, 723–743. [https://doi.org/10.1016/S0306-4522\(96\)00485-X](https://doi.org/10.1016/S0306-4522(96)00485-X) (1997).
44. Trapp, S., Tucker, S. J. & Gourine, A. V. Respiratory responses to hypercapnia and hypoxia in mice with genetic ablation of Kir5.1 (Kcnj16). *Exp. Physiol.* **96**, 451–459. <https://doi.org/10.1113/expphysiol.2010.055848> (2011).
45. Wellner-Kienitz, M. C., Shams, H. & Scheid, P. Contribution of Ca²⁺-activated K⁺ channels to central chemosensitivity in cultivated neurons of fetal rat medulla. *J. Neurophysiol.* **79**, 2885–2894. <https://doi.org/10.1152/jn.1998.79.6.2885> (1998).
46. Zhu, G. *et al.* CO₂ inhibits specific inward rectifier K⁺ channels by decreases in intra- and extracellular pH. *J. Cell. Physiol.* **183**, 53–64. [https://doi.org/10.1002/\(sici\)1097-4652\(200004\)183:1%3c53::aid-jcp7%3e3.0.co;2-r](https://doi.org/10.1002/(sici)1097-4652(200004)183:1%3c53::aid-jcp7%3e3.0.co;2-r) (2000).
47. Cohen, N. A., Brenman, J. E., Snyder, S. H. & Brecht, D. S. Binding of the inward rectifier K⁺ channel Kir 2.3 to PSD-95 is regulated by protein kinase A phosphorylation. *Neuron* **17**, 759–767. [https://doi.org/10.1016/S0896-6273\(00\)80207-X](https://doi.org/10.1016/S0896-6273(00)80207-X) (1996).
48. Choi, J. E., Lyons, K. M., Kieser, J. A. & Waddell, N. J. Diurnal variation of intraoral pH and temperature. *BDJ Open* **3**, 17015–17015. <https://doi.org/10.1038/bdopen.2017.15> (2017).
49. Dickman, R. *et al.* Relationships between sleep quality and pH monitoring findings in persons with gastroesophageal reflux disease. *J. Clin. Sleep Med.* **3**, 505–513 (2007).
50. Xiong, J., Lan, L., Lian, Z. & De Dear, R. Associations of bedroom temperature and ventilation with sleep quality. *Sci. Technol. Built Environ.* **26**, 1274–1284 (2020).
51. Ayas, N. T., Brown, R. & Shea, S. A. Hypercapnia can induce arousal from sleep in the absence of altered respiratory mechanoreception. *Am. J. Respir. Crit. Care Med.* **162**, 1004–1008. <https://doi.org/10.1164/ajrccm.162.3.9908040> (2000).
52. Magalhães, K. S. *et al.* Locus Coeruleus as a vigilance centre for active inspiration and expiration in rats. *Sci. Rep.* **8**, 15654. <https://doi.org/10.1038/s41598-018-34047-w> (2018).
53. Aston-Jones, G., Gonzalez, M. & Doran, S. Role of the locus coeruleus-norepinephrine system in arousal and circadian regulation of the sleep–wake cycle. *Brain norepinephrine: Neurobiology and therapeutics*, 157–195. <https://www.researchwithrutgers.com/en/publications/role-of-the-locus-coeruleus-norepinephrine-system-in-arousaland-fingerprints/?sortBy=alphabetically> (2007).
54. Breton-Provencher, V. & Sur, M. Active control of arousal by a locus coeruleus GABAergic circuit. *Nat. Neurosci.* **22**, 218–228. <https://doi.org/10.1038/s41593-018-0305-z> (2019).
55. Reinoso-Barbero, F. & de Andrés, I. Effects of opioid microinjections in the nucleus of the solitary tract on the sleep-wakefulness cycle states in cats. *Anesthesiology* **82**, 144–152. <https://doi.org/10.1097/0000542-199501000-00019> (1995).
56. Souza, G. M. P. R., Stornetta, R. L., Stornetta, D. S., Abbott, S. B. G. & Guyenet, P. G. Contribution of the retrotrapezoid nucleus and carotid bodies to hypercapnia- and hypoxia-induced arousal from sleep. *J. Neurosci.* **39**, 9725–9737. <https://doi.org/10.1523/jneurosci.1268-19.2019> (2019).
57. Grace, K. P., Hughes, S. W., Shahabi, S. & Horner, R. L. K⁺ channel modulation causes genioglossus inhibition in REM sleep and is a strategy for reactivation. *Respir. Physiol. Neurobiol.* **188**, 277–288. <https://doi.org/10.1016/j.resp.2013.07.011> (2013).
58. Brooks, P. L. & Peever, J. H. Identification of the transmitter and receptor mechanisms responsible for REM sleep paralysis. *J. Neurosci.* **32**, 9785–9795. <https://doi.org/10.1523/jneurosci.0482-12.2012> (2012).
59. Ballanyi, K., Onimaru, H. & Homma, I. Respiratory network function in the isolated brainstem-spinal cord of newborn rats. *Progr. Neurobiol.* **59**, 583–634. [https://doi.org/10.1016/S0301-0082\(99\)00009-X](https://doi.org/10.1016/S0301-0082(99)00009-X) (1999).
60. Jiang, N. *et al.* Obstructive sleep apnea and circulating potassium channel levels. *J. Am. Heart Assoc.* <https://doi.org/10.1161/jaha.116.003666> (2016).
61. Alomri, R. M., Kennedy, G. A., Wali, S. O., Ahejaili, F. & Robinson, S. R. Differential associations of hypoxia, sleep fragmentation, and depressive symptoms with cognitive dysfunction in obstructive sleep apnea. *Sleep* <https://doi.org/10.1093/sleep/zsaa213> (2021).
62. Ding, F. *et al.* Changes in the composition of brain interstitial ions control the sleep-wake cycle. *Science* **352**, 550–555. <https://doi.org/10.1126/science.aad4821> (2016).
63. Kumar, T. & Jha, S. K. Influence of cued-fear conditioning and its impairment on NREM sleep. *Neurobiol. Learn. Mem.* **144**, 155–165. <https://doi.org/10.1016/j.nlm.2017.07.008> (2017).

Acknowledgements

This work was supported by grants from the Department of Science and Technology-CSRI Grant Numbers: DST-CSRI 2021/136 (G); DST-CSRI/39/2016(G)] funded to Sushil K Jha. We also acknowledge the funding from SERB, DBT-BUILDER and Department of Science and Technology-(PURSE).

Author contributions

F.A.M. performed and designed the experiments, analyzed the data, and prepared the manuscript. S.K.J. conceived and conceptualized the ideas, designed the experiments, analyzed the data, and finalized the manuscript. All authors reviewed the manuscript before submission.

Competing interests

The authors declare no competing interests.

Additional information

Supplementary Information The online version contains supplementary material available at <https://doi.org/10.1038/s41598-024-71818-0>.

Correspondence and requests for materials should be addressed to S.K.J.

Reprints and permissions information is available at www.nature.com/reprints.

Publisher's note Springer Nature remains neutral with regard to jurisdictional claims in published maps and institutional affiliations.

Open Access This article is licensed under a Creative Commons Attribution-NonCommercial-NoDerivatives 4.0 International License, which permits any non-commercial use, sharing, distribution and reproduction in any medium or format, as long as you give appropriate credit to the original author(s) and the source, provide a link to the Creative Commons licence, and indicate if you modified the licensed material. You do not have permission under this licence to share adapted material derived from this article or parts of it. The images or other third party material in this article are included in the article's Creative Commons licence, unless indicated otherwise in a credit line to the material. If material is not included in the article's Creative Commons licence and your intended use is not permitted by statutory regulation or exceeds the permitted use, you will need to obtain permission directly from the copyright holder. To view a copy of this licence, visit <http://creativecommons.org/licenses/by-nc-nd/4.0/>.

© The Author(s) 2024